The effects of hydrogen sulfide on the polymer electrolyte membrane fuel cell anode catalyst: H_2S–Pt/C interaction products

Thiago Lopes*, Valdecir A. Paganin, Ernesto R. Gonzalez

Instituto de Química de São Carlos, Universidade de São Paulo, PO Box 780, São Carlos, São Paulo 13560-970, Brazil

ABSTRACT

The performance of a polymer electrolyte membrane fuel cell (PEMFC) operating on a simulated hydrocarbon reformate is described. The anode feed stream consisted of 80% H_2, ∼20% N_2, and 8 ppm hydrogen sulfide (H_2S). Cell performance losses are calculated by evaluating cell potential reduction due to H_2S contamination through lifetime tests. It is found that potential, or power, loss under this condition is a result of platinum surface contamination with elemental sulfur. Electrochemical mass spectroscopy (EMS) and electrochemical techniques are employed, in order to show that elemental sulfur is adsorbed onto platinum, and that sulfur dioxide is one of the oxidation products. Moreover, it is demonstrated that a possible approach for mitigating H_2S poisoning on the PEMFC anode catalyst is to inject low levels of air into the H_2S-contaminated anode feeding stream.

© 2011 Elsevier B.V. All rights reserved.

1. Introduction

Polymer electrolyte membrane fuel cells (PEMFCs) have commonly been regarded as the most promising energy conversion units for a sustainable world. Over the last two decades, they have been extensively studied and developed to the point of being close to entering the mass market. Despite being already sold by a few companies worldwide, these attractive alternatives are still more expensive than internal combustion engines, for instance. Among the barriers to their widespread commercialization are the relatively high cost and limited durability of their components. There are many degradation and failure mechanisms within a PEMFC system [1]. Impurities or contaminants are one of the factors that may lead to premature cell failure, because they can enter the cell together with the feeding gases, thereby affecting functioning of vital cell components, such as catalysts and membrane. Contaminant is a species that negatively affects any membrane electrode assembly (MEA) component, and, thus, cell performance. Reaction rate contaminants are species that adsorb onto the active site, hence blocking the catalyst for the desired reaction. This blockage reduces catalyst active surface available for reaction and gives rise to over-

potentials at the electrode. Overpotentials at the anode and/or the cathode, in turn, reduce cell potential, and thus cell efficiency. So for fuel cells to be implemented in the mass market, it is crucial that the effects of any reaction rate contaminant on the MEA components be known.

One example of reaction rate contaminant is the well known case of carbon monoxide (CO) [1–7]. There is also hydrogen sulfide (H_2S), which has received considerably less attention, though [8–14]. Hydrogen sulfide is a gaseous acid at ambient temperature and pressure, and it has strong affinity for metals, especially metal oxides, such as, platinum oxides. Thereby making PEM fuel cells sensitive to H_2S.

Natural gas is one of the primary hydrogen sources and, depending on the geographic region of extraction, it may contain large H_2S amounts (up to several vol.%). Other fossil fuels, such as gasoline, also have a number of sulfur-containing compounds, like thiophene, thiols, and carbon sulfide. These sulfurous compounds are converted to H_2S during natural gas and fossil fuel reforming for hydrogen production [15], so H_2S can reach the cell anode and consequently the platinum catalyst.

Mohtadi et al. [13] have investigated the influence of cell temperature on the extent of PEMFC contamination by H_2S, in the 50–90 °C range. These authors concluded that catalyst contamination is faster at higher temperatures. This tendency was also observed by Chin and Howard [16] on a phosphoric acid fuel cell. Murthy et al. [11] have also studied the influence of H_2S on PEMFC performance and concluded that, in contrast with cases involving CO-contamination, the presence of ruthenium in the catalyst (PtRu/C) did not make it any more tolerant to H_2S. Knights et al.

* Corresponding author. Present address: Departamento de Química, Faculdade de Filosofia, Ciências e Letras de Ribeirão Preto, Universidade de São Paulo, Postal Code: 14040-901, Ribeirão Preto, São Paulo, Brazil. Tel.: +55 16 36023784; fax: +55 16 36332660.
E-mail addresses: tlopeschem@gmail.com (T. Lopes), ernesto@iqsc.usp.br (E.R. Gonzalez).

[12] have examined a PEMFC operating at 80 °C, 100 mA cm^{-2}, and exposed to 1.2 ppm H$_2$S. A 300 mV reduction in the cell potential was detected after 25 h of contamination. The later authors also studied the same system at 500 mA cm^{-2}, but exposed to 0.1 ppm H$_2$S, and they observed a 250 mV decrease in cell potential after 300 h of exposure to the contaminant. Electrode potential scan is regularly employed to remove sulfur species from the platinum catalyst [8–16].

Voltammograms for sulfur removal display two oxidation peaks, one at a more positive and another at a less positive potential, which correspond to the presence of two different adsorbed species, distinguished by the number of occupied platinum sites, i.e., one (linear-bonded) or two (bridge-bonded) [17]. Bernardi et al. [18] and Yourong et al. [19] have investigated platinum nanoparticles sulfidation by X-ray photoelectron spectroscopy and X-ray absorption spectroscopy, and they concluded that the sulfur species adsorbed/bonded onto the catalyst is elemental sulfur, which is bound to the metal at higher sulfidation temperatures but is adsorbed to the metal at lower temperatures. Analyzing the results, from these investigations, it can be expected that sulfur is adsorbed and not bound to platinum nanoparticles in the temperature range where PEMFCs operate. This important information suggests that H$_2$S interacts with the PEMFC catalyst through chemical dissociation, which generates hydrogen and elemental sulfur. Mathieu and Primet [20] have studied H$_2$S chemisorption onto Pt–Al$_2$O$_3$ and reported that H$_2$S adsorbs dissociatively onto platinum, generating elemental sulfur and gaseous hydrogen.

Loučka [21] carried out the first investigation on the kinetics of H$_2$S adsorption and oxidation on platinum electrodes in aqueous phase. He showed that H$_2$S becomes completely dehydrogenated upon adsorption onto platinum electrodes, and that the amount of charge associated with adsorbed sulfur oxidation was too high to account for the oxidation of a mere monolayer of adsorbed sulfur. The excess charge was attributed to formation of a poorly reducible oxide on the electrode. In the light of the research accomplished by Bernardi et al. [18], this extra charge can be ascribed to oxidation of elemental sulfur that was place-exchanged in the metal lattice. These place-exchanged atoms are formed during the contamination process and can be present in the second and third atomic layers [18]. According to Loučka [21], the complete adsorbed sulfur removal by oxidation cannot be reached just by holding the poisoned Pt electrode at a potential as high as 1600 mV vs SHE, unless the sulfur coverage degree on the electrode is very low. However, complete sulfur removal can be achieved by periodically polarizing the electrode to such positive potentials. Loučka has proposed the following mechanism for the oxidation process:

$$Pt–S + 3H_2O \leftrightarrow SO_3 + 6H^+ + 6e^- + Pt \qquad (1.1)$$

$$Pt–S + 4H_2O \leftrightarrow SO_2^4 + 8H^+ + 6e^- + Pt \qquad (1.2)$$
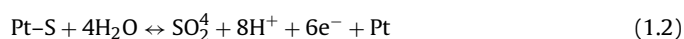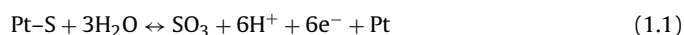
For H$_2$S chemical dissociation on the platinum surface, one can also propose the following mechanism described by Mathieu and Primet [20]:

$$Pt + 4H_2S \leftrightarrow Pt–S + H_2 \qquad (1.3)$$

$$Pt–H + H_2S \leftrightarrow Pt–S + 3/2H_2 \qquad (1.4)$$

And the following mechanism can be proposed for H$_2$S electrochemical oxidation on Pt:

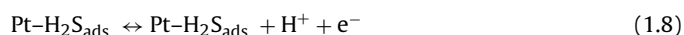$$Pt + H_2S \leftrightarrow Pt–S_{ads.} + 2H^+ + 2e^- \qquad (1.5)$$
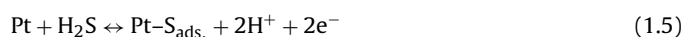
Farooque et al. [22,23] have looked into H$_2$S electrochemical oxidation on platinum surfaces by using a rotating tripolar wiper-blade electrode in the low potential region of 0–450 mV vs SHE [22], and in the Tafel potential region, 450–1400 mV vs SHE [23]. These authors demonstrated that in the lower oxidation potential

region, the anodic H$_2$S oxidation follows a two-electron process, to yield elemental sulfur, protons, and electrons. Using a statistical tool to validate the most likely model, the authors concluded that H$_2$S oxidation follows the mechanism given below in the lower potential region:

Chemical reaction:

$$Pt + H_2S \leftrightarrow Pt–H_2S_{ads.} \qquad (1.6)$$

$$Pt + SH^- \leftrightarrow Pt–SH_{ads.} \qquad (1.7)$$

Electrochemical reaction:

$$Pt–H_2S_{ads.} \leftrightarrow Pt–H_2S_{ads.} + H^+ + e^- \qquad (1.8)$$

$$Pt–SH_{ads.} \leftrightarrow Pt–S_{ads.} + H^+ + e^- \qquad (1.9)$$

which confirms the two-electron mechanism put forward by Loučka.

Many investigations into the interaction between H$_2$S and platinum have been concluded. Such studies involved the gaseous [13,16,20,24–27] and aqueous [17,19,21–23,28–32] phases. In the gas phase, sulfur formation by a dissociative chemical reaction was found to take place, which also produces H$_2$. However, in the aqueous phase H$_2$S is oxidized on the platinum electrode through a two electron reaction, which produces protons and elemental sulfur.

PEMFC electrodes have a three-phase boundary or a mixture of gaseous and aqueous phases. Thus, the contaminant reaches both phases during PEMFC contamination with H$_2$S. Therefore, a mixture of gaseous and aqueous phase Pt–H$_2$S interaction products is expected. However, there are no spectroscopic data to clarify this prediction in literature. In this context, the aim of the present paper is to clarify that both product phases are indeed present.

Regarding the elemental sulfur oxidation products on platinum electrodes, they are expected to be SO$_2$, SO$_3$ and/or SO$_4^{2-}$ [21,33]. However, they have not been monitored in PEMFCs by spectroscopic techniques yet. So a second aim of this work is to identify the adsorbed sulfur oxidation products on platinum in the case of PEMFCs.

2. Experimental

Standard gas diffusion electrodes were prepared by applying a mixture of carbon powder (Vulcan XC-72, Cabot) and 15% (w/w) polytetrafluoroethylene solution (PTFE, TE-306, DuPont) onto both faces of a carbon cloth substrate (PWB-3, Stackpole). The loading (carbon + PTFE, C/PTFE = 8.5:1.5) was 3 mg cm^{2-} per face. The catalyst layer was composed of a homogeneous suspension formed by 0.1 mL Nafion^{TM} solution (Aldrich, 5 wt.%), 9.24 mg 20% Pt/C (E-TEK) electrocatalyst, and 0.05 mL isopropanol. This suspension was homogenized in an ultrasonic bath for 10 min, with subsequent solvent evaporation. The resulting solid material was dispersed again in isopropanol, to produce an ink, which was quantitatively deposited by a brushing procedure onto one face of the composite diffusion layer [34]. The membrane and electrode assemblies (MEAs) were obtained by hot-pressing two electrodes (4.62 cm^2 each) on both sides of a pre-treated Nafion^{TM} 117 membrane (H$^+$, DuPont) [34] at 125 °C and 5 MPa, for 2 min. The MEA was placed between high-density carbon plates, in which serpentine-type gas distribution channels were machined. The nominal catalyst loading on both electrodes was 0.4 mg Pt cm^{-2}. Fuel cell polarization measurements were carried out on a galvanostat (Electronic Load HP 6050A). The cell was kept at 80 °C, under pure O$_2$ (99.5%) flow passing through water at 85 °C, and pure H$_2$ (99.99%) flow passing through water at 95 °C. The simulated hydrocarbon reformate gas consisted of a mixture of H$_2$ (99.99%) 80% in vol. + N$_2$/40 ppm H$_2$S (99.5% in N$_2$) 20% in vol. and was used as the fuel stream during the contamination procedure. The cell was maintained at
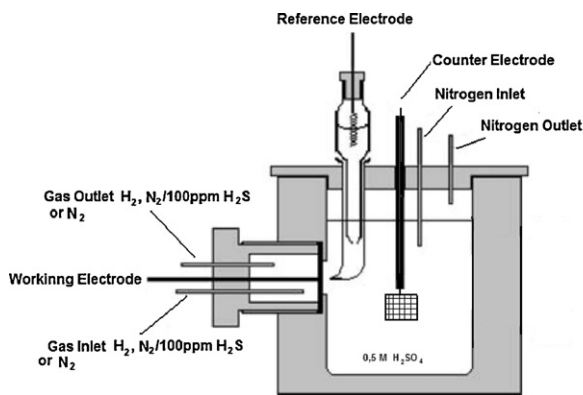
Fig. 1. Electrochemical cell utilized for experiments with platinum-catalyzed gas-diffusion electrodes in a 0.5 M sulfuric acid solution.

700 mV for 2 h, under pure H_2 and O_2 flow, before every experiment. The gas diffusion electrodes employed in the three-electrode cell experiments were prepared according to a literature procedure [34], except for the C/PTFE ratio, which was 7:3 in our case. Electrochemical experiments were accomplished with a cell manufactured in PTFE (Fig. 1). The reactant gases were N_2 (99.99%), H_2 (99.999%) and N_2/40 ppm H_2S (99.5% in N_2) (White Martins). The electrolyte was 0.5 M H_2SO_4. The geometric area of the working electrode exposed to the electrolyte was 1.23 cm². A platinum mesh was used as counter electrode, and the reversible hydrogen electrode was employed as reference. Electrochemical tests were conducted using a Solartron 1285A potentiostat/galvanostat, and the current was measured as a function of time or voltage. The experiments were performed under atmospheric pressure and room temperature. An electrochemical mass spectrometer (EMS) was utilized for monitoring of the products generated from H_2S interaction with platinum, and the EMS was also used to confirm the chemical and electrochemical formation of elemental sulfur in PEMFCs and to identify the sulfur oxidation product during cyclic voltammetry/potential scan. The gas outlet of the three-electrode cell (Fig. 1) was connected to the mass spectrometer GSD 301 Omnistar from Pfeiffer Vacuum, so as to follow the H_2S–Pt/C interaction products online. This same procedure was employed on the PEMFC anode

gas outlet, in order to track the sulfur oxidation products during cyclic voltammetry/potential scan for platinum surface regeneration. The EMS gas analysis system consisted of a quadrupole (QMS 200, Prisma), containing a Faraday cup and a secondary electron multiplier (SEM) as ion detectors. It is noteworthy that the EMS capillary, connected to the anode outlet, was kept at 105 °C during the experiments on the PEMFC, to prevent water condensation.

3. Results and discussion

PEM fuel cell lifetime tests were carried out, to access the H_2S effects on cell performance. A simulated hydrocarbon reformate (hydrogen-rich gas) was used as fuel during the lifetime tests. This hydrogen rich gas was periodically contaminated with H_2S 8 ppm, but the contamination period varied according to the objective of each experiment. Fig. 2 depicts the huge voltage loss caused by the presence of the contaminant in the fuel stream. The cell potential loss was 224 mV within 1.78 h of exposure.

Many authors [8,9,11–13,15] have observed the same trend upon PEMFC exposure to H_2S, even when the latter is present at lower levels (0.1 ppm) than those investigated herein. As discussed in Section 1, cell performance losses are associated with either anode catalyst poisoning or platinum active sites blockage. The contaminant deactivates a fraction of the catalyst surface and diminishes the hydrogen oxidation reaction (HOR) rate. This reduction produces overpotentials on the anode electrode, thereby decreasing the cell potential difference. The H_2S amount that passes from the anode to the cathode compartment through the membrane is very low [35], so, it can be considered that the cathode potential remains unchanged during the contamination process.

After the contamination, H_2S was purged from the anode electrode by using pure nitrogen, followed by cyclic voltammetry. Typical voltammograms are presented in Fig. 2. Submitting the electrode to potential scans removes almost all the sulfur species formed during the contamination of the catalyst surface. The sulfur species adsorbed onto the platinum surface are seen in the voltammograms as two oxidation peaks, Fig. 3, which correspond to the oxidation of elemental sulfur adsorbed onto platinum through one (linear-bound) and two (bridge-bound) metal atoms [17]. From the voltammograms in Fig. 3, it was possible to calculate the fraction of
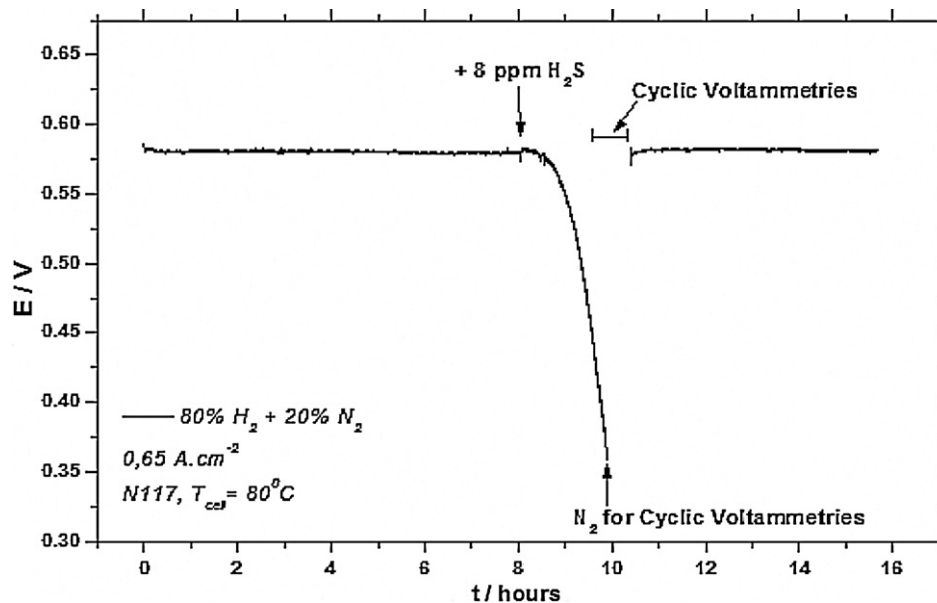

Fig. 2. Lifetime test depicting PEMFC performance before and during exposure to 8 ppm H_2S in the fuel stream (1.78 h), and after cyclic voltammetries (4 and 5 cycles) for sulfur removal. Cell current density, 650 mA cm⁻² cell temperature, 80 °C, catalyst, 20% Pt/C E-TEK, membrane, N117.
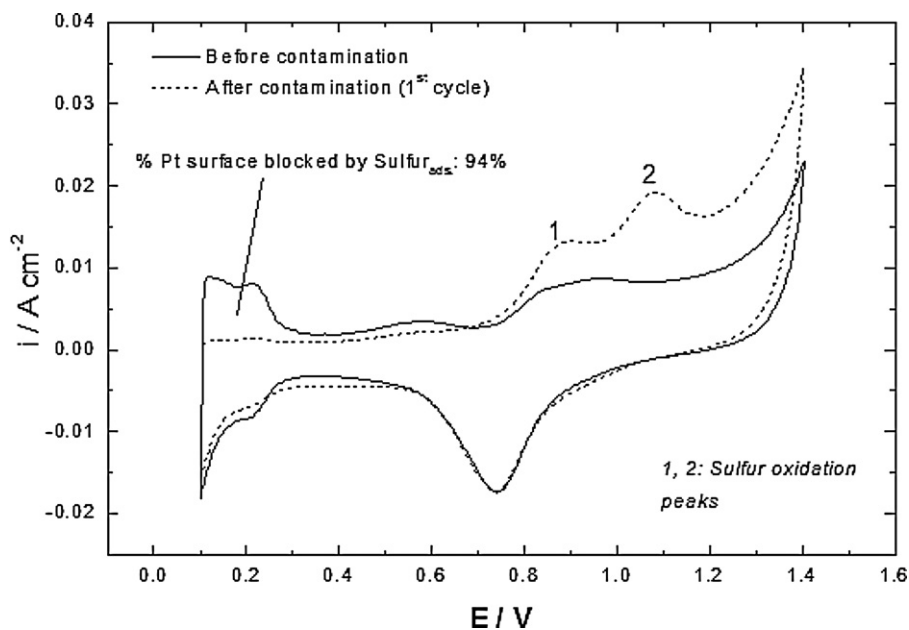
Fig. 3. PEMFC anode voltammogram profile before and after exposure to 8 ppm H_2S for 1.78 h. Scan rate, 20 mV s^{-1}.

catalyst surface that was deactivated. This calculation showed that 94% of the platinum surface area was inaccessible for hydrogen oxidation after the contamination process.

A second lifetime test was performed with the same parameters, except for the current density and exposure time, which were 380 mA cm^{-2} and 2.78 h, respectively. These changes elevated the initial cell potential to approximately 690 mV and reduced the catalyst surface contamination level to 78%, Table 1.

Table 1 lists data extracted from the lifetime tests and cyclic voltammograms. Analysis of these data suggests that overpotentials are present on the anode electrode, once changes in current density culminate in higher catalyst surface contamination. This can be explained by the fact that modifications in the initial cell potential only should not affect the contamination level, and that all cell potential drops associated with enhanced cell current density are mainly related to cathode overpotentials. Chin et al. [16] have contaminated a phosphoric acid fuel cell with H_2S and also observed that the poisoning extent increased as a function of the electrode potential. In order to confirm that overpotentials exist on our anode electrode, experiments were accomplished in a three-electrode electrochemical cell (Fig. 1) with a platinum-catalyzed gas-diffusion electrode that was placed in contact with a sulfuric acid solution. Fig. 4 displays the voltammograms for hydrogen oxidation registered before and after exposure of the working electrode to 100 ppm H_2S/N_2 for 1200 s at two different adsorption potentials, 16 mV and 25 mV vs RHE, in a stripping experiment resembling those performed for carbon monoxide oxidation investigations [5]. This cell configuration was preferred because it enables better electrode potential control while it still consisted of the same PEMFC electrode (gas-diffusion electrode) and contained the same three-phase boundary. Fig. 4 reveals that increasing electrode potential during the H_2S adsorption step resulted in overpotentials for hydrogen oxidation. This clearly confirms that increments in cell current density give rise to anode overpotentials and consequently to higher degradation rates in the case that PEMFC is fed with H_2S-contaminated hydrogen.

The same three-electrode electrochemical cell configuration (Fig. 1) employing a platinum-catalyzed gas diffusion electrode as working electrode was coupled to an EMS, in order to detect the reaction products generated on the anode electrode during PEMFC
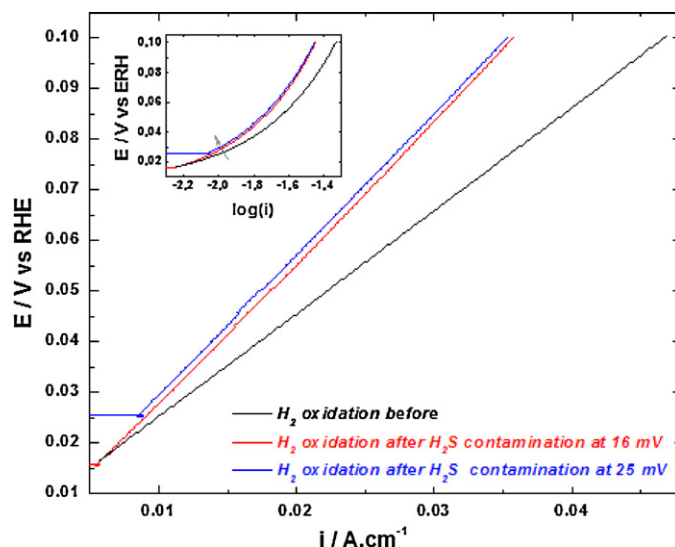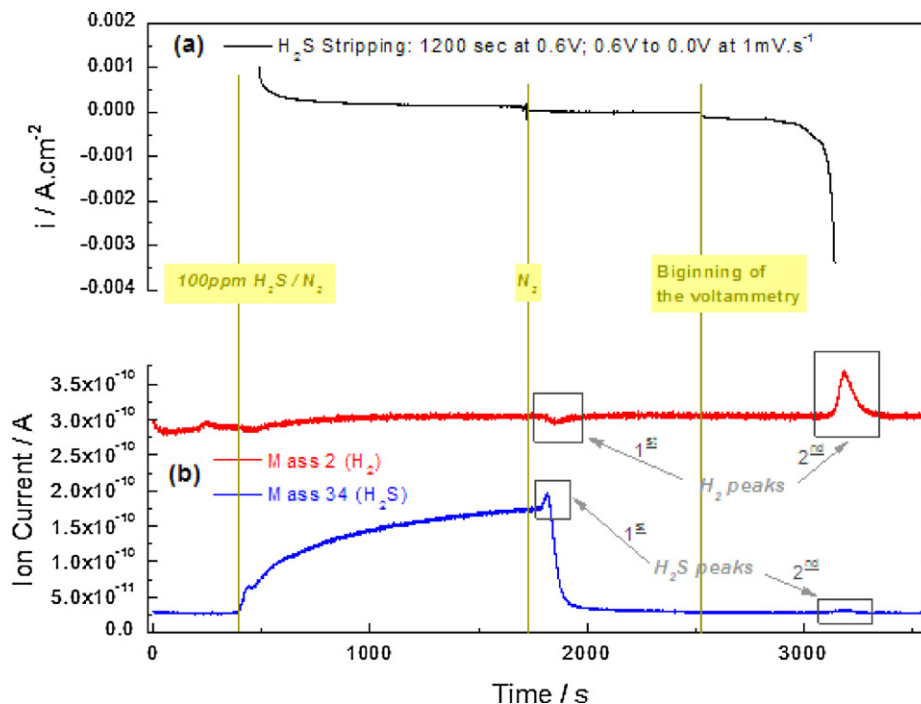

Fig. 4. Hydrogen oxidation linear sweep voltammograms on platinum-catalyzed gas-diffusion electrodes, in a three electrode electrochemical cell, Fig. 1. Platinum loading, 0.4 mg$_{Pt}$ cm^{-2}, 0.5 M H_2SO_4 solution, room temperature, scan rate, 1 mV s^{-1}. Hydrogen oxidation performed before and after electrode exposure to 100 ppm H_2S/N_2 for 1200 s at 16 mV and 25 mV vs RHE.

contamination with H_2S. In this case, another CO stripping-like experiment was performed, where the H_2S adsorption potential was 600 mV vs RHE. After 1200 s of H_2S adsorption (100 ppm H_2S/N_2), the electrode potential was scanned down to 0 mV vs RHE, at 1 mV s^{-1}, under pure N_2 flow (Fig. 5a). Fig. 5b represents the relative intensity of masses 2 and 34, or H_2 and H_2S, respectively. The relative intensity assigned to H_2 increased continuously during the H_2S adsorption at 600 mV vs RHE, indicating that H_2S interacts with platinum through a dissociative chemical reaction. It is noteworthy that a fraction of the generated H_2 was oxidized on the electrode at this high potential. However, due to the high gas flow rate, another fraction reached the EMS and could be detected. From Fig. 5b it is apparent that when the 100 ppm H_2S/N_2 flow was interrupted, or when the H_2S chemical potential in the gas phase

Table 1
Summary of data extracted from lifetime tests for PEMFC performance analysis during exposure to 8 ppm H_2S.

| j ($A cm^{-2}$)	$t_{contamination}$ (h)	$E_{initial}$ (mV)	E_{final} (mV)	ΔE_{cell} (mV)	$Pt_{contaminated}^{Surface}$ (%)	Sulfur oxidation charge $[Q_{01} + Q_{02}]$ (Coulombs)
0.65	1.78	582	358	−224	94	7.575E−5
0.38	2.78	692	498	−194	78	6.523E−5

Fig. 5. (a) H_2S stripping voltammetry: H_2S adsorbed at 600 mV vs RHE (1200 s) for further potential scan from 600 mV to 0 mV vs RHE at 1 mV s^{-1} in pure N_2 atmosphere; (b) EMS relative current intensities of masses 2 and 34, or H_2 and H_2S, respectively. Measured during H_2S stripping voltammetry. Room temperature.

was drastically reduced, a negative peak arose at the H_2 relative intensity, which was associated with a positive peak at the H_2S relative intensity. Fig. 5b also evidences that when the electrode potential was close to zero, a second peak appeared at the H_2S relative intensity during the scan. In this potential region, hydrogen production on the electrode took place, so its chemical potential in the gas phase was higher. These data are clearly described by reactions (1.3) and (1.4). In turn, reduction in the H_2S chemical potential in the gas phase drove reactions (1.3) and (1.4) back to the reactants, or to $Pt + H_2S$ and $Pt–H + H_2S$, consuming hydrogen. Increments in hydrogen chemical potential in the gas phase also drove reactions (1.3) and (1.4) back to the reactants, generating H_2S. Fig. 5a depicts the electrochemical part of the experiment, where positive currents were detected during H_2S adsorption at 600 mV vs RHE (disregarding double layer charging). In contrast, no currents were observed when pure nitrogen was purged through the electrode, but negative currents were noticed when the electrode potential was scanned down to 0 mV vs RHE at 1 mV s^{-1}. Negative currents should be analyzed in the double layer potential region only, since at lower potentials negative currents are due to hydrogen generation. These data confirm that H_2S is oxidized/reduced on platinum-catalyzed gas-diffusion electrodes. Furthermore, Fig. 3 indicates that H_2S is oxidized to elemental sulfur and protons (Eqs. (1.8) and (1.9)). It is apparent, therefore, that the products from the H_2S–Pt/C interaction investigated in applied science fundamental studies [13,16,17,19–32], are both present on a PEMFC electrode. In other words, our results demonstrate that H_2S interacts with PEMFC platinum anodes through a dissociative chemical reaction (Eqs. (1.3) and (1.4)) and through an electrochemical oxidative reaction (Eqs. (1.8) and (1.9)).

In order to indentify the oxidation products of sulfur adsorbed onto platinum in the PEMFC anode, the anode gas outlet was connected to the EMS, and the gaseous products were monitored during the potential scan/cyclic voltammetry. Fig. 6 reveals that the SO_2 relative intensity increases during the potential scan of the sulfur-contaminated PEMFC anode. Therefore, it is probable that one of the sulfur oxidation products is sulfur dioxide. As water is present in this three-phase boundary electrode, sulfate (SO_4^{2-}) is another expected product, besides SO_3, whose signal could not be distinguished from that of SO_2. Loučka [21] proposed that sulfate would be a product of sulfur oxidation on platinum electrodes, which was later observed by Wang et al. [31] in aqueous phase experiments through X-ray photoelectron spectroscopy.

After the cyclic voltammetry experiments, hydrogen was set back to flow on the anode electrode, which prompted high hydrogen chemical potential in the reaction compartment and augmented the H_2 relative intensity (Fig. 6). However, a large peak also appeared at the H_2S relative intensity. From these results, it is apparent that the dissociative chemical reaction is an important mechanism in the recovery process. It is also possible that the anode potential scan alone does not account for catalyst surface regeneration and sulfur removal. Uribe et al. [36] have investigated the performance recovery of a H_2S-contaminated PEMFC concerning interruption of the contaminant flux and the flow of pure hydrogen through the anode electrode. They came to the conclusion that this process is not able to reestablish the PEMFC performance. The present work does not intend to clarify this more fundamental question. However, our experimental observations point to the following hypothesis: in the reduction part of the sulfur oxidation voltammogram, sulfide (S^{2-}) could be formed, and the S^{2-} species
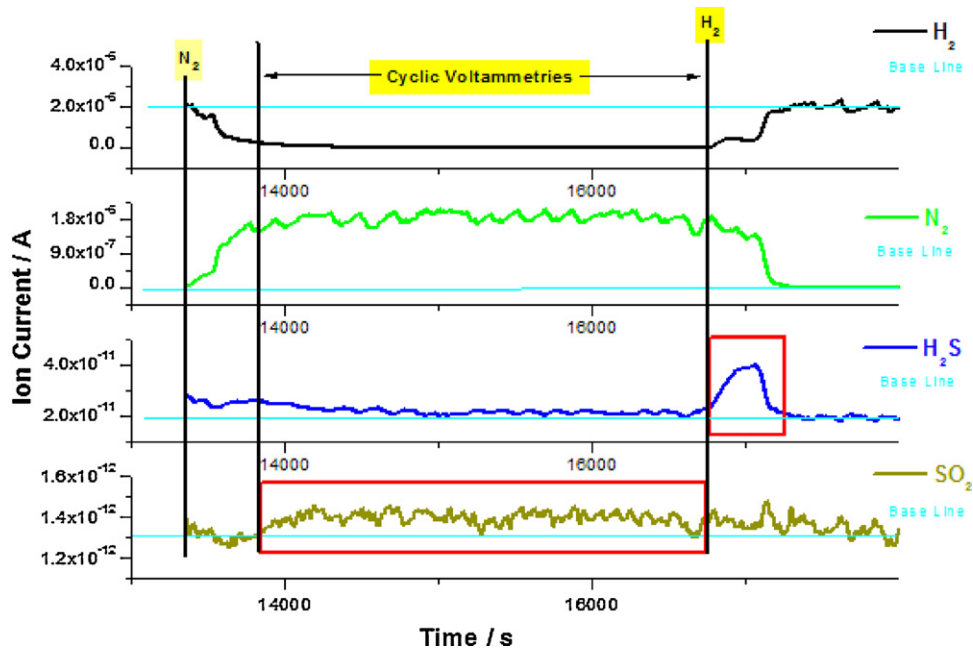
Fig. 6. EMS relative current intensities of masses 2, 28, 34 and 64 or H_2, N_2, H_2S and SO_2, respectively measured during cyclic voltammetries after the lifetime test depicted in Fig. 2.

together with H^+ generated during hydrogen oxidation could react, to form H_2S again. In this way, the contaminant should be completely removed from the catalyst surface.

The electrode potential scan technique is a widely used method for PEMFC performance recovery after H_2S contamination. Nevertheless, it results in cell performance degradation, which is a cumulative process, Fig. 7. This has been attributed to Pt agglomeration, due to the loss of metal–support interaction [26,27] induced by sulfur adsorption. An alternative explanation to this performance loss is the formation of platinum sulfides and oxides that are difficult to reduce [33]. On the base of the oxygen and sulfur place-exchange properties [37], which can be found in the sec-

ond and third atomic layers of platinum nanoparticles [18], and bearing in mind that few cycles (4 and 5) were performed during each cleaning process (cyclic voltammetry) in the present investigation two hypotheses can be formulated, presented in order of importance. The first is that during the electrode potential scan, the removal of place-exchanged sulfur atoms causes structural changes in the nanoparticle [18], thereby resulting in particle growth and loss of contact with the support [26,27], with consequent PEMFC performance loss. The second hypothesis is that a fraction of place-exchanged sulfur atoms in the nanocrystal probably is not removed from the catalyst by the potential scan, culminating in catalyst activity loss.
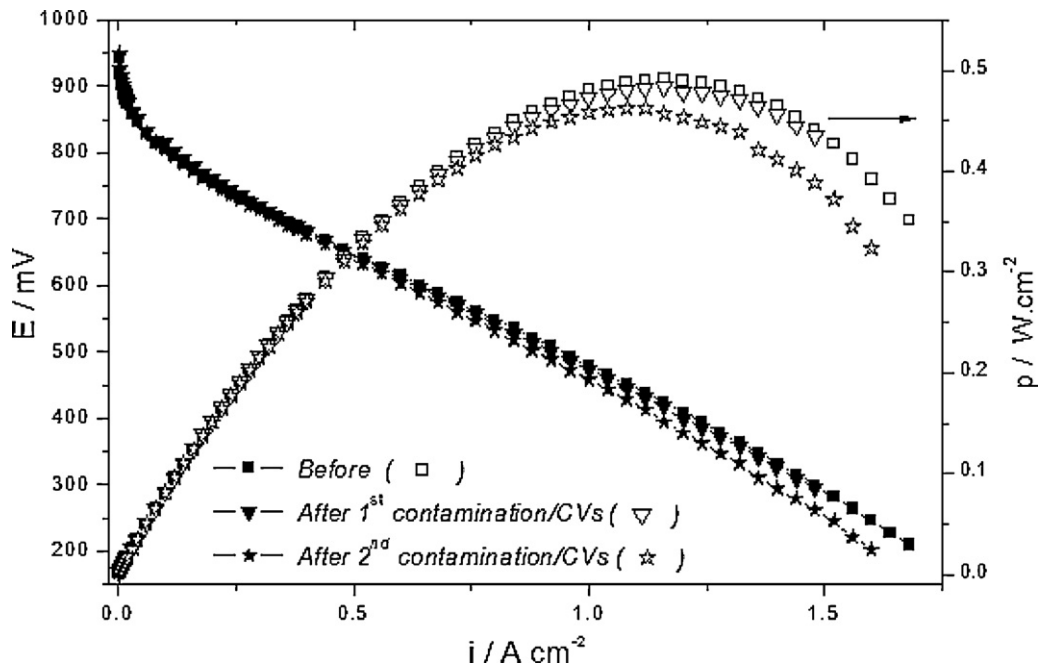
Fig. 7. Polarization (solid symbols) and power density (open symbols) plots of a PEMFC before and after consecutive contamination/sulfur removal cycles. Contamination performed by 8 ppm $H_2S/(80\% H_2 + 20\% N_2)$ for 1.78 h with cell current density at 650 mA cm^{-2}, N117, 80 °C.
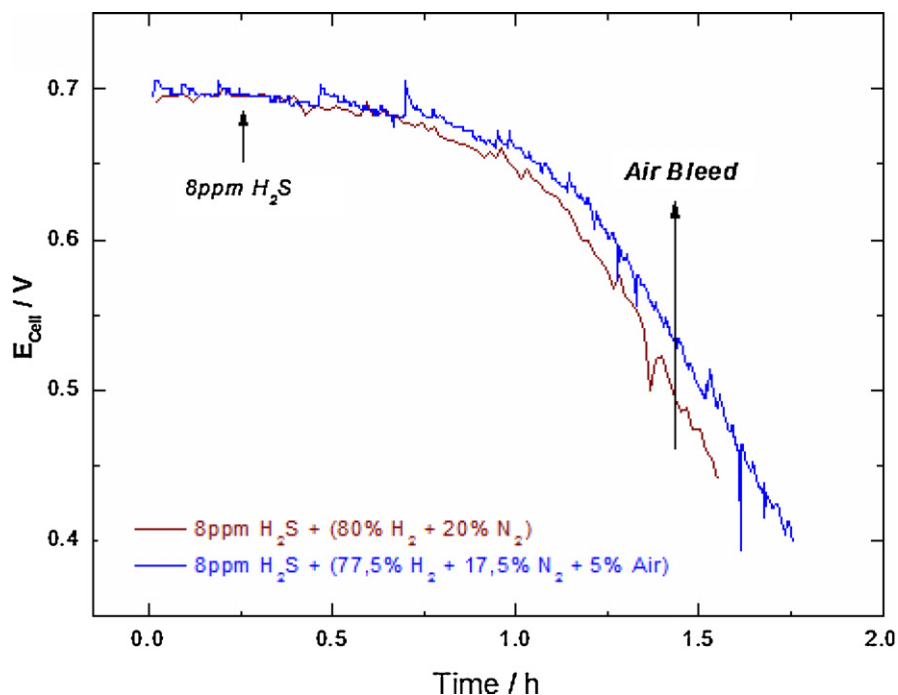
Fig. 8. Lifetime tests of a PEMFC exposed to 8 ppm H_2S for 1.8 h with and without 5% air in the fuel stream (air-bleed). Cell current density, 380 mA cm^{-2}, cell temperature 80 °C, catalyst, 20% Pt/C from E-TEK.

This undesired side effect prompted by the electrode potential scanning, led us to test the well-known *air-bleed* technique [1], which was developed for PEMFC contamination with CO, and has an important advantage over cyclic voltammetry: it is not necessary to shout the cell down. Our observation that SO_2 is a sulfur oxidation product was another reason for employing such technique. Because part of the sulfur adsorbed onto the catalyst surface undergoes oxidation to SO_2, it was considered that sulfur may be oxidized to sulfur dioxide in the presence of oxygen (*air-bleed*), as in the case of CO. This would decontaminate the catalyst, once excess hydrogen flowed through the anode compartment. We propose the following reaction scheme for the process:

$$H_2S + (1\%)O_2 + 3Pt \leftrightarrow Pt-S + 2Pt-O \qquad (3.1)$$

$$Pt-S + 2Pt-O \leftrightarrow SO_2 + 3Pt \qquad (3.2)$$
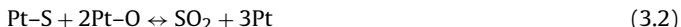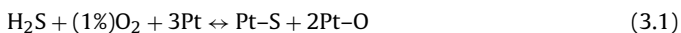
Lifetime tests (Fig. 8) were recorded for *air-bleed* tests during H_2S contamination of a PEMFC, and there is evidence that this technique promoted cell tolerance to sulfur. However, the observed tolerance was not as significant as that obtained for CO contamination of PEMFCs [1]. As discussed above, this smaller tolerance is probably due to the fact that the amount of SO_2 generated during the sulfur oxidation represented a small fraction of the total. Another explanation, less likely but possible, is the fact that SO_2 also poisons PEMFC platinum anodes [38]. Taken together, these data highlight the need for developing catalysts that present tolerance to H_2S.

4. Conclusions

PEMFC performance loss is detected when these cells are operated on a simulated hydrocarbon reformate contaminated with 8 ppm H_2S. The fraction of platinum surface contaminated with sulfur increases with cell current density. Overpotentials for hydrogen oxidation arise on the platinum-catalyzed gas-diffusion electrode as a function of the H_2S adsorption potential, in the three-electrode cell. This explains the increments in catalyst surface contamination with elevated cell current density and proves that there are

overpotentials for HOR on the PEMFC anode electrode. EMS data suggest that H_2S adsorbs onto PEMFC platinum electrodes via dissociation, thereby, generating elemental sulfur, adsorbed onto the catalyst surface, and H_2. Electrochemical experiments indicate that H_2S interacts with the platinum catalyst oxidatively, producing elemental sulfur and H^+. EMS data of a single PEMFC cell evidence that SO_2 is a sulfur oxidation product that is generated during the anode electrode potential scan. Polarization curve analysis shows that cyclic voltammetry is not the best technique for re-establishing the performance of a H_2S-contaminated PEMFC. The *air-bleed* method, in turn, is an alternative technique that confers sulfur tolerance to PEMFCs.

References

[1] S. Gottesfeld, T.A. Zawodzinski, in: R.C. Alkire, H. Gerischer, D.M. Kolb, C.W. Tobias (Eds.), Advances in Electrochemical Science and Engineering, vol. 5, John Wiley, 1998, p. 195.
[2] J. St. Pierre, in: F.N. Büchi, M. Inaba, T.J. Schmidt (Eds.), Polymer Electrolyte Fuel Cell Durability, Springer, New York, NY, 2009, p. 289.
[3] K. Ruth, M. Vogt, R. Zuber, in: W. Vielstich, A. Lamm, H.A. Gasteiger (Eds.), Handbook of Fuel Cells: Fundamentals, Technology and Applications, vol. 3, John Wiley & Sons, 2003, p. 489.
[4] D.P. Wilkinson, J. St-Pierre, in: W. Vielstich, A. Lamm, H.A. Gasteiger (Eds.), Handbook of Fuel Cells: Fundamentals, Technology and Applications, vol. 3, John Wiley & Sons, 2003, p. 611.
[5] T. Iwasita, E.G. Ciapina, in: W. Vielstich, H. Yokkawa, H.A. Gasteiger (Eds.), Handbook of Fuel Cells: Fundamentals, Technology and Applications, vol. 5, John Wiley & Sons, 2009, p. 224.
[6] T. Madden, M. Perry, L. Protsailo, M. Gummalla, S. Burlatsky, N. Cipollini, S. Motupally, T. Jarvi, in: W. Vielstich, H. Yokkawa, H.A. Gasteiger (Eds.), Handbook

of Fuel Cells: Fundamentals, Technology and Applications, vol. 6, John Wiley & Sons, 2009, p. 861.

[7] B. Du, R. Pollard, J.F. Elter, M. Ramani, in: F.N. Büchi, M. Inaba, T.J. Schmidt (Eds.), Polymer Electrolyte Fuel Cell Durability, Springer, New York, NY, 2009, p. 341.

[8] F.H. Garzon, F.A. Uribe, in: W. Vielstich, H. Yokkawa, H.A. Gasteiger (Eds.), Handbook of Fuel Cells: Fundamentals, Technology and Applications, vol. 5, John Wiley & Sons, 2009, p. 264.

[9] H.W. Benz, F. Mahlendorf, O. Niemzig, J. Roes, Fuel Cell Seminar 2002 Extended Abstracts, Palm Springs, CA, USA, 2002, p. 149.

[10] Z. Shi, D. Song, J. Zhang, Z.-S. Liu, S. Knights, R. Vohra, N.-Y. Jia, D. Harvey, J. Electrochem. Soc. 154 (2007) B609.

[11] R. Mohtadi, W.-K. Lee, S. Cowan, J.W. Van Zee, M. Murthy, Electrochem. Solid-State Lett. 6 (2003) A272.

[12] S. Knights, N. Jia, C. Chuy, J. Zhang, 2005 Fuel Cell Seminar Extended Abstracts, Palm Springs, CA, USA, 2005, p. 121.

[13] R. Mohtadi, W.K. Lee, J.W. Van Zee, Appl. Catal. B: Environ. 56 (2005) 37.

[14] T. Gu, W.-K. Lee, J.W. Van Zee, M. Murthy, J. Electrochem. Soc. 151 (2004) A2100.

[15] R. Borup, J. Meyers, B. Pivovar, Y.S. Kim, R. Mukundan, N. Garland, D. Myers, M. Wilson, F. Garzon, D. Wood, P. Zelenay, K. More, K. Stroh, T. Zawodzinski, J. Boncella, J.E. McGrath, M. Inaba, K. Miyatake, M. Hori, K. Ota, Z. Ogumi, S. Miyata, A. Nishikata, Z. Siroma, Y. Uchimoto, K. Yasuda, K.-I. Kimijima, N. Iwashita, Chem. Rev. 107 (2007) 3904.

[16] D.T. Chin, P.D. Howard, J. Electrochem. Soc. 133 (1986) 2447.

[17] A.Q. Contractor, H. Lal, J. Electroanal. Chem. 96 (1979) 175.

[18] F. Bernardi, M.C.M. Alves, A. Traverse, D.O. Silva, C.W. Scheeren, J. Dupont, J. Morais, J. Phys. Chem. C 113 (2009) 3909.

[19] W. Yourong, Y. Heqing, W. E'feng, J. Electroanal. Chem. 497 (2001) 163.

[20] M.V. Mathieu, M. Primet, Appl. Catal. 9 (1984) 361.

[21] T. Loučka, J. Electroanal. Chem. 31 (1971) 319.

[22] M. Farooque, T.Z. Fahidy, J. Electrochem. Soc. 124 (1977) 1191.

[23] M. Farooque, T.Z. Fahidy, J. Electrochem. Soc. 125 (1978) 544.

[24] R. Mohtadi, W-k. Lee, S. Cowan, J.W. Van Zee, M. Murthy, Electrochem. Solid-State Lett. 6 (2003) A272.

[25] Z. Paal, K. Matusek, M. Muhler, Appl. Catal. A 149 (1997) 113.

[26] J.R. Chang, S.L. Chang, T.B. Lin, J. Catal. 169 (1997) 338.

[27] J.R. Chang, S.L. Chang, J. Catal. 176 (1998) 42.

[28] E. Najdeker, E. Bishop, J. Electroanal. Chem. 41 (1979) 79.

[29] E. Lamy-Pitara, L. Bencharif, J. Barbier, Electrochem. Acta 30 (1985) 971.

[30] E. Lamy-Pitara, Y. Tainon, B. Beden, J. Barbier, J. Electroanal. Chem. 279 (1990) 291.

[31] Y. Wang, H. Yan, E. Wang, J. Electroanal. Chem. 497 (2001) 163.

[32] Y. Wang, H. Yan, E. Wang, Sens. Actuators B 87 (2002) 115.

[33] V.A. Sethuraman, L.A. Wise, S. Balasubramanian, J.W. Weidner, ECS Trans. 1 (2006) 111.

[34] V.A. Paganin, E.A. Ticianelli, E.R. Gonzalez, J. Appl. Electrochem. 26 (1996) 297.

[35] E.L. Brosha, T. Rockward, F.A. Uribe, F.H. Garzon, ECS Trans. 17 (2009) 369.

[36] F.A. Uribe, T.A. Zawodzinski Jr., 200th ECS Meeting, San Francisco, Fall, 2001 (Abstract #339).

[37] B.E. Conway, Prog. Surf. Sci. 49 (1995) 331.

[38] T. Lopes, E.R. Gonzalez, Quim. Nova 31 (2008) 551.